Cellular Signalling 63 (2019) 109387

Contents lists available at ScienceDirect

Cellular Signalling

journal homepage: www.elsevier.com/locate/cellsig

MeCP2 triggers diabetic cardiomyopathy and cardiac fibroblast proliferation by inhibiting RASSF1A

Hui Tao[a], Jun-Ye Tao[a], Zheng-Yu Song[a], Peng Shi[b], Qin Wang[a], Zi-Yu Deng[c], Xuan-Sheng Ding[a,*]

[a] School of Basic Medical Sciences and Clinical Pharmacy, China Pharmaceutical University, Nanjing 210009, PR China
[b] Department of Cardiothoracic Surgery, The Second Hospital of Anhui Medical University, Hefei 230601, PR China
[c] The Second Hospital of Anhui Medical University, Hefei 230601, PR China

ARTICLE INFO

Keywords:
Methyl CpG binding protein 2
Diabetes cardiomyopathy
Proliferation
Cardiac fibroblasts
Ras association domain family 1 isoform A

ABSTRACT

Diabetes causes cardiomyopathy and increases the risk of heart failure independent of hypertension and cardiac fibrosis disease. However, the molecular mechanism of cardiomyopathy caused by diabetic (DCM) is currently unknown. Here we explore the role of the Methyl CpG binding protein 2 (MeCP2) in DCM patients and a type 1 DM (T1DM) rat model. In this study, we employed streptozotocin (STZ)-induced rats DCM and DCM patient and found that MeCP2 triggers cardiac fibroblast proliferation in DCM by inhibiting of RASSF1A expression. Moreover, the in vitro study demonstrated that high glucose inhibited RASSF1A expression, accompanied by the increases of MeCP2 expression and DNA hypermethylation in RASSF1A promoter region. MeCP2 inhibition or knockdown reversed the decrease of RASSF1A transcription induced by high glucose in cardiac fibroblasts. MeCP2 triggers cardiac fibroblasts proliferation through the activation of RASSF1A/ERK1/2 signaling pathways. Our results demonstrated that MeCP2 plays a key role in RASSF1A mediated ERK1/2 activation in DCM. Taken together, these indicate that MeCP2 acts as a key regulator of DCM and cardiac fibroblasts proliferation.

1. Introduction

Diabetic cardiomyopathy (DCM) is an important contributor to morbidity and mortality of diabetic patients by causing heart failure. Cardiac fibrosis plays a crucial role in DCM [1]. The abnormal proliferation of cardiac fibroblasts and deposition of the extracellular matrix (ECM) results in cardiac fibrosis development, which then adversely affects the performance of the heart [2]. Moreover, cardiac fibroblasts proliferation is associated with increasing in collagen I and smooth muscle α-action (α-SMA) expression [3]. However, there is limited information regarding the pathological mechanism of cardiac fibroblasts proliferation and DCM.

It is known that the Ras/ERK1/2 signal pathway activation is induced in activated cardiac fibroblasts and triggers proliferation [4]. Ras association domain family 1 isoform A (RASSF1A) is a methylation thereof that can negatively regulate Ras/ERK1/2 pathway [5]. Suppressing ERK1/2 pathway inhibits collagen deposition and proliferation in activated cardiac fibroblasts [6]. RASSF1A has been found to be inactivated by promoter methylation in fibrosis disease [7,8]. However, little is known about how RASSF1A change in DCM and cardiac fibroblasts proliferation.

Gene silencing can be regulated by DNA methylation [9,10]. Methyl CpG binding protein 2 (MeCP2) may specifically bind to methylated DNA sequences in the genome [11,12]. The protein encoded by the MeCP2 gene contains a methyl-CpG binding domain (MBD) and a transcriptional repression domain (TRD) [13]. MeCP2 as a transcription repressor, acting by binding to the methylated sequences of its target gene promoter and leading to gene silencing [14]. Recent studies indicated that MeCP2 plays a key role in fibrosis and cell proliferation.

However, MeCP2 triggers diabetic cardiomyopathy and cardiac fibroblast proliferation by suppressing RASSF1A has not been investigated. Given the role of RASSF1A in mediating ERK1/2 activation

Abbreviations: MeCP2, Methyl CpG binding protein 2; MBD, methyl-CpG binding domain; T1DM, type 1 DM; ECM, Extracellular matrix; α-SMA, α-smooth muscle actin; STZ, Streptozotocin; RASSF1A, Ras association domain family 1 isoform A; 5-AzadC, 5-aza-2′-deoxycytidine; TRD, Transcriptional repression domain; HDACs, Histone deacetylases

* Corresponding author at: School of Basic Medical Sciences and Clinical Pharmacy, China Pharmaceutical University, Nanjing, Jiangsu Province 210009, PR China.
E-mail address: dxs0162@sina.com (X.-S. Ding).

https://doi.org/10.1016/j.cellsig.2019.109387
Received 27 April 2019; Received in revised form 13 June 2019; Accepted 5 August 2019
Available online 06 August 2019
0898-6568/

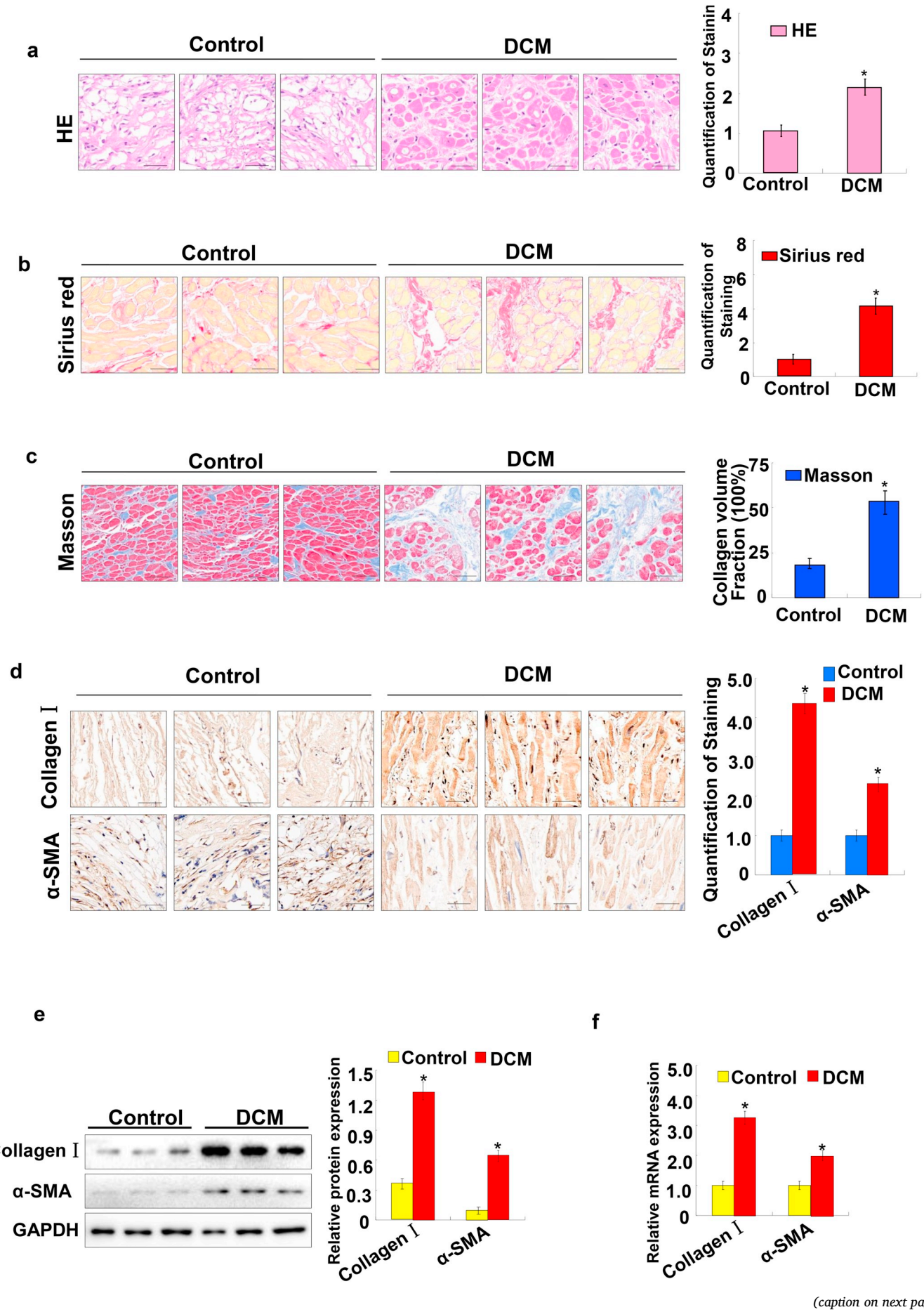

(caption on next page)

Fig. 1. Distinction of DCM patients and fibrosis phenotypic changes.
Thin sections were cut and stained with hematoxylin and eosin (H&E) (a), Sirius Red stain (b), Masson's trichrome stain (c). Scale bar, 50 μm. Patients were grouped health (control) hearts or DCM patient hearts. (d) CollagenIand α-SMA immunostaining on sections of health (control) hearts or DCM patient hearts. (e) The relative CollagenIand α-SMA expression levels were detected by Western blotting. (f) The relative CollagenIand α-SMA expression levels were detected by qRT-PCR. Data are representative of at least three separate experiments. *p < .05, **p < .01 vs control. (For interpretation of the references to colour in this figure legend, the reader is referred to the web version of this article.)

[15], we hypothesized that RASSF1A plays an important role in regulating ERK1/2 activation associated with cardiac fibroblasts proliferation. In this article, we investigated that MeCP2 triggers diabetic cardiomyopathy and cardiac fibroblast proliferation through suppressing RASSF1A mediated ERK1/2 activation.

2. Materials and methods

2.1. Reagents

Streptozotocin (STZ) was purchased from Sigma (Sigma, St. Louis, MO). Mouse monoclonal antibodies for α-SMA, Collagen I were purchased from Boster (Wuhan, China), MeCP2 polyclonal antibody were purchased from Abcam (Cambridge, UK). RASSF1A, ERK1/2, p-ERK1/2 antibodies were purchased from Cell Signaling (Beverly, MA, U.S.A.). MeCP2, RASSF1A, α-SMA, collagen I primers were produced by the Shanghai Sangong Biological and Technological Company (Shanghai, China). Immunohistochemical kit was obtained from the Zhongshan Biotechnology Corporation (Beijing, China). Secondary antibodies were obtained from Santa Cruz Biotechnology (Santa Cruz, California, USA).

2.2. Animal models

All experiments were performed in accordance with the National Institutes of Health Guidelines on the Use of Laboratory Animals and approved by the China Pharmaceutical University Committee on Animal Care. Fifty adult male Sprague-Dawley rats weighing 180–220 g by using streptozotocin (STZ) injection strategy as indicated previously [16,17]. DCM rat model was produced by common STZ as previously described [17]. 12 weeks later, the animals were anesthetized, killed and their hearts were harvested. Heart tissue specimens were fixed in 4% phosphate-buffered paraformaldehyde. Other heart tissue specimens were snap-frozen in liquid nitrogen and stored at −80 °C for RNA and protein analysis.

2.3. Human myocardium samples

Samples from patients with diabetic cardiomyopathy and healthy subjects were obtained from the Second Affiliated Hospital of Anhui Medical University. Following consent, heart tissue from patients with diabetic cardiomyopathy and non-diabetes were obtained at the time of underwent heart valve replacement surgery or cardiac catheterization. This study received approval from the ethical committee of Anhui Medical University, and written informed consent was obtained from all patients.

2.4. Cell culture and treatment with glucose

Cardiac fibroblasts (CFs) were harvested from SD neonate rats and cultured. Cells were collected and were passaged for 48 h and serum-starved with 0.5% FCS for 24 h before adding 5.5 mM glucose (Control) or 33.3 mM glucose (HG). Cardiac fibroblasts were cultured on plastic in DMEM (Gibco, U.S.A.), supplemented with 100 U/ml penicillin, 100 mg/ml streptomycin, 2 mM L-Glutamine, and 10% fetal calf serum, respectively. Cell cultures were maintained at 37 °C in an atmosphere of 5% CO_2.

2.5. MTT assay

Cells (5×10^3/ml) were cultured with various concentrations of glucose for 24 h in 96-well plates. After culture, 5 mg/ml MTT (Sigma) reagent was added and incubated for 4 h at 37 °C before adding DMSO to dissolve formazan crystals and measuring in triplicate at 490 nm wavelength using a Thermomax microplate reader (bio-tekEL, U.S.A.).

2.6. CCK-8 assay

Cell proliferation was studied using CCK-8 (Dojindo Laboratories, Japan). After treatment, cells were seeded in six-well plates at approximately 1000 per well. After being cultured for 24 h, cells were

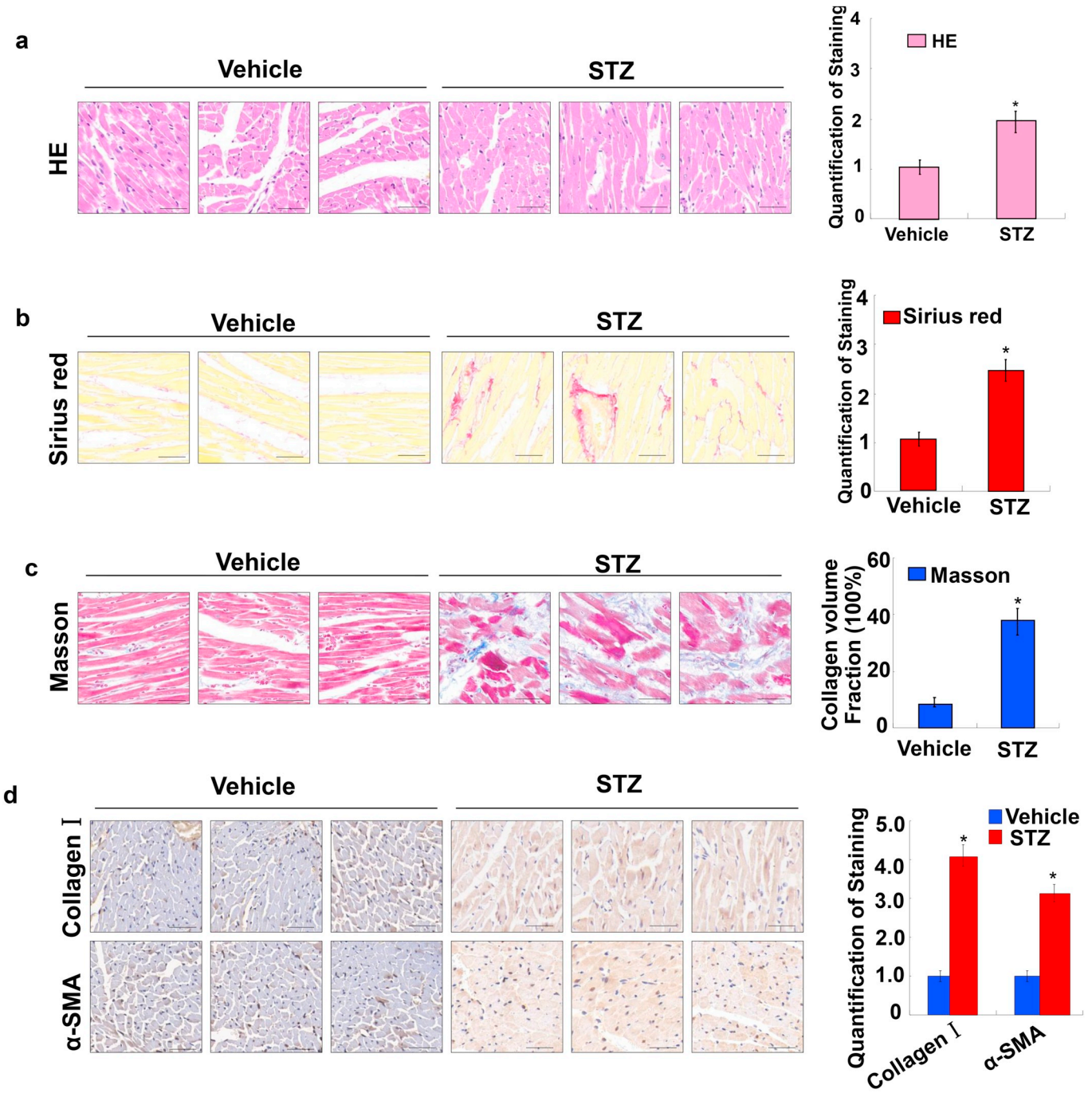

(caption on next page)

Fig. 2. STZ-induced rat display symptoms of DCM and fibrosis.
Thin sections were cut and stained with hematoxylin and eosin (H&E) (a), Sirius Red stain (b), Masson's trichrome stain (c). Scale bar, 50 μm. Rats were grouped control (vehicle) hearts or STZ-rat DCM hearts. (d) CollagenIand α-SMA immunostaining on sections of control (vehicle) hearts or STZ-rat DCM hearts. (e) The relative CollagenIand α-SMA expression levels were detected by Western blotting. (f) The relative CollagenIand α-SMA expression levels were detected by qRT-PCR. Data are representative of at least three separate experiments. *p < .05, **p < .01 vs vehicle. (For interpretation of the references to colour in this figure legend, the reader is referred to the web version of this article.)

added in 10 ml CCK-8 solutions. After incubating for 2 h, the OD value was measured at 450 nm wavelengths using a Thermomax microplate reader (bio-tekEL, USA).

2.7. DNA content and cell cycle analysis

After treatment, cells were fixed in 70% ice-cold ethanol and stored at 4 °C for 24 h. After centrifugation, cells were rehydrated in PBS and stained with propidium iodide (PI) solution (50 μg/ml) containing RNase A (100 μg/ml). PI stained cells were analyzed for DNA content in a BD FACS Array (BD Biosciences, Piscataway, NJ, USA). The results were treated with ModFit LT 3.0 (Verity Software House, Topsham, ME, USA).

2.8. Histological analysis

Hematoxylin and eosin (HE) staining, Sirius Red staining and Masson's trichrome staining. Tissue from the heart fixed in 4% paraformaldehyde were embedded in paraffin and cut into 5-μm thick sections. The sections were stained separately with HE, Sirius Red staining and Masson's trichrome. The morphology of the cardiomyocytes and the deposition of collagen were observed by fluorescence microscope.

2.9. Immunohistochemistry

Every paraffin-embedded sample was sectioned 5 μm thick and laid out on polylysine-coated slides. According to the immunohistochemical assay manufacturer's protocol. Heart tissue sections were deparaffinized and rehydrated and stained with primary antibodies against: rat polyclonal anti-MeCP2 (1:100), anti-α-SMA (1:50) and anti-CollagenI(1:50). Then incubated with the secondary antibody for 1 h at room temperature. At least five random fields of each section were examined, and semiquantitative evaluations were analyzed with a Photo and Image Auto analysis System (Image-pro-plus, China).

2.10. Immunofluorescence staining

Paraffin-embedded heart sections and cultured cardiac fibroblasts were incubated with antibodies (anti-MeCP2 1:50, anti-α-SMA 1:100, anti-RASSF1A 1:50) overnight at 4 °C. The following day, the tissue sections and cells were incubated with the appropriate secondary antibodies for 30 min at 37 °C. All sections were counterstained with 4′-6-diamidino-2-phenylindole (DAPI, Invitrogen). Specific fluorescence was acquired by laser-scanning confocal microscopy (LSM710, Carl Zeiss, Germany).

2.11. RNA interference analysis

RNAi experiments in cardiac fibroblasts were performed by forward transfection in 48 h of cultured cardiac fibroblasts using Lipofectamine™2000 (Invitrogen) according to the manufacturer's protocol. Small interfering RNA (siRNA) oligonucleotides against MeCP2 genes or scrambled sequences were synthesized by the Shanghai GenePharma Corporation. The following siRNA sequences were used: si-MeCP2 (rat), 5′-GGGACCUAUGUAUGAUGACTT-3′ (sense) and 5′-GUCAUCA UACAUAGGUCCCTT-3′ (anti-sense); The following siRNA sequences were used: si-RASSF1A (rat), 5′-CCAAAUAUACUUCCGGAA ATT-3′ (sense) and 5′-UUUC CGGAAGUAUAUUUGGTT-3′ (anti-sense); si-control with a scrambled sequence (negative control siRNA having no perfect matches to known rat genes), 5′-UUCUCCGAACGUGUCACG UTT-3′ (sense) and 5′-ACGUGACACGUUCG GAGAATT-3′ (antisense). Transfection was allowed to proceed for various times and cells were processed for different assays. The siRNA transfection efficiency of Lipofectamine™2000 in cells was determined by the BLOCK-IT Alexa Fluor Red Fluorescent Oligo protocol (Invitrogen).

2.12. Plasmid constructions and transfection

For over-expression, the MeCP2 cDNA was amplified through PCR,

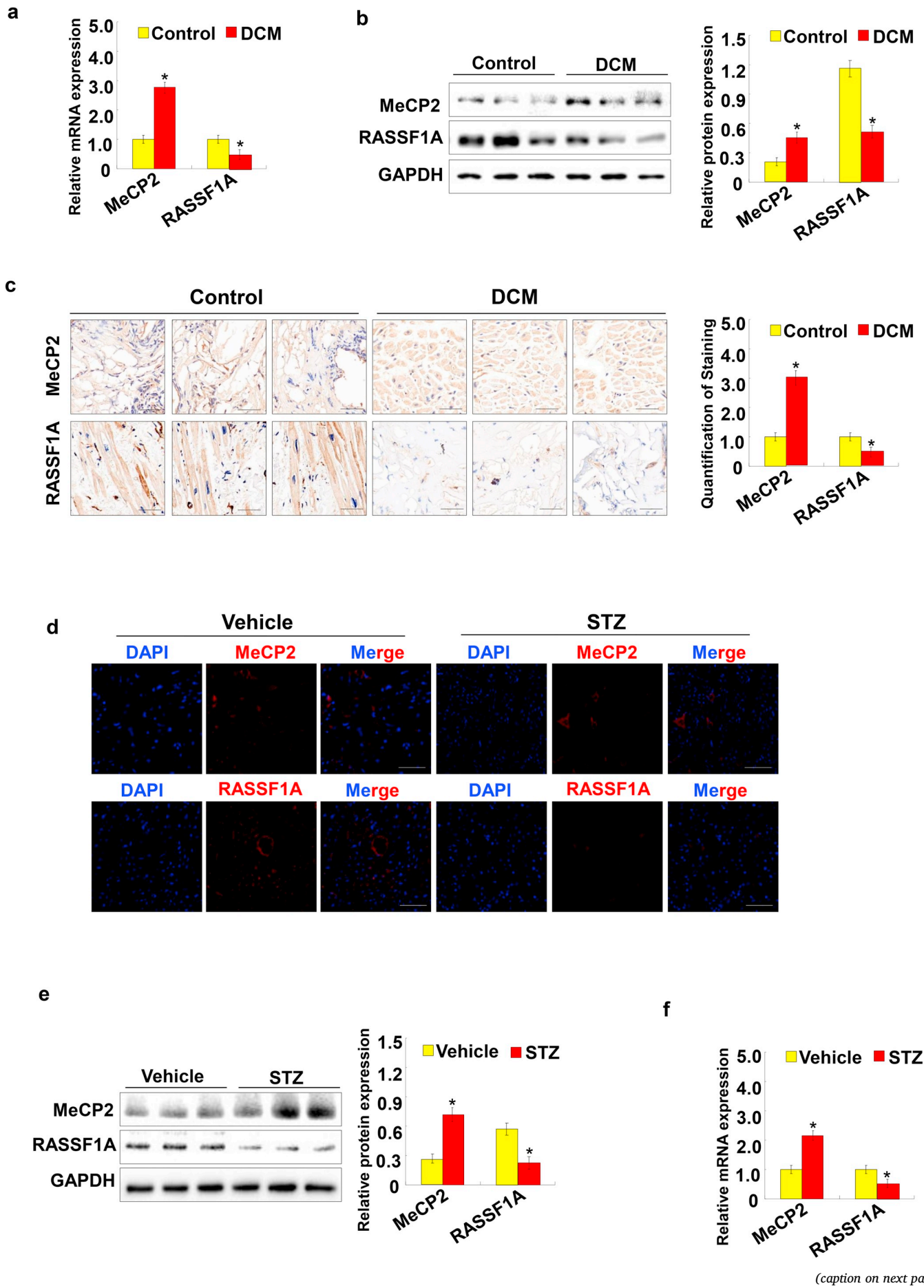

(caption on next page)

Fig. 3. Differential expressions of MeCP2 and RASSF1A in DCM patient and STZ-induced DCM hearts. (a) The relative MeCP2 and RASSF1A mRNA expression levels in DCM patient were detected by qRT-PCR. (b) The relative MeCP2 and RASSF1A protein expression levels in DCM patient were detected by Western blotting. (c) The relative MeCP2 and RASSF1A protein immunostaining on sections of control (vehicle) hearts or DCM patient hearts. (d) Immunofluorescence analysis MeCP2 and RASSF1A protein immunostaining on sections of control (vehicle) hearts or STZ-rat DCM hearts. MeCP2 and RASSF1A, red; nuclei, blue. Scale bar, 50 μm. (e) The relative MeCP2 and RASSF1A expression levels were detected by Western blotting. (f) The relative MeCP2 and RASSF1A expression levels were detected by qRT-PCR. Data are representative of at least three separate experiments. *$p < .05$, **$p < .01$ vs vehicle or control. (For interpretation of the references to colour in this figure legend, the reader is referred to the web version of this article.)

inserted into the pEGFP-C1 vector to generate pEGFP-C1-MeCP2 and subsequently sequence. The plasmid containing MeCP2 was transfected using Lipofectamine 2000 (Invitrogen, CA, USA) according to the manufacturer's protocol. The cells were transfected with a linearize pEGFP-C1-MeCP2 or a linearize empty vector using Lipofectamine 2000 (Invitrogen).

2.13. RNA preparation and analysis

Total RNA was extracted from heart tissues and cardiac fibroblasts using TRIzol reagents (Invitrogen). The RNA was reverse transcribed using a reverse transcription kit. The cDNA was amplificated and detected by the ABI 7500 Fast Real-Time PCR system (Applied Biosystems, CA, USA). The primers for MeCP2, RASSF1A, α-SMA, Collagen I and GAPDH were purchased from the Shanghai Sangong Corporation. PCR was performed at 95 °C for 10 min followed by 40 cycles at 95 °C for 15 s and at 60 °C for 1 min. The cycle threshold (CT value) of the target genes was normalized to that of GAPDH to obtain the delta CT (ΔCT). The ratio of the relative expression of target genes to GAPDH was calculated by using the 2ΔCT formula. The sequences of primers are listed as follows. α-SMA Forward 5′ TGG CCACTGCTGCTTCCTCTTCTT 3′, Reverse 5′ GGGGCCAGCTTCGTCATACTC CT 3′; MeCP2 Forward 5′ CAGCT CCAACAGGATTCCATGGT 3′, Reverse 5′ AGGCAGGCA AAGCAGA GACATCA 3′; CollagenI Forward 5′ TACAGCACG CTTGTGG ATG3′, Reverse 5′ TTGAGTTTGGGTTGTTGGTC 3′; RASSF1A Forward 5′ GAGACACCTGATCTTTCCCA 3′, Reverse 5′ CTGGAAGG CACTG AAACA 3′; GAPDH Forward 5′ AGTGCCAGCCTCGTCTCATAG 3′, Reverse 5′ ACTGTGCCGTTGAACTTGCC 3′.

2.14. Western blotting

Heart tissues and cardiac fibroblasts were lysed with lysis buffer (Beyotime, China). Total proteins from samples of interest were then fractionated by electrophoresis through a 10% SDS-PAGE. Gels ran at a 120 V for 1.5 h before transferring onto a PVDF membrane. After blockade of nonspecific protein binding, nitrocellulose blots were incubated for 1 h with primary antibodies diluted in TBS/Tween20. Antibody to MeCP2, RASSF1A, α-SMA, Collagen I, ERK1/2, p-ERK1/2 and GAPDH was diluted in 1:200–1:1000. Membranes were then washed extensively with TBS/T and incubated with a secondary antibody (1:5000) (Santa Cruz Biotechnology, USA) for 1 h at room temperature. Proteins were visualized using the ECL Plus detection system (GE Healthcare, WI, USA). Band intensity was quantified by gel densitometry with the Gel Image Analysis System (UVP).

2.15. Statistical analysis

Quantitative data are expressed as mean ± SD. Statistical significance was determined by either the Student's *t*-test for comparison between means or one-way analysis of variance with a post hoc Dunnett's test. If $p < .05$, the result was considered to be statistically significant.

3. Results

3.1. The fibrosis phenotypic changes in DCM patients

To investigate the distinction of DCM patients and health control.

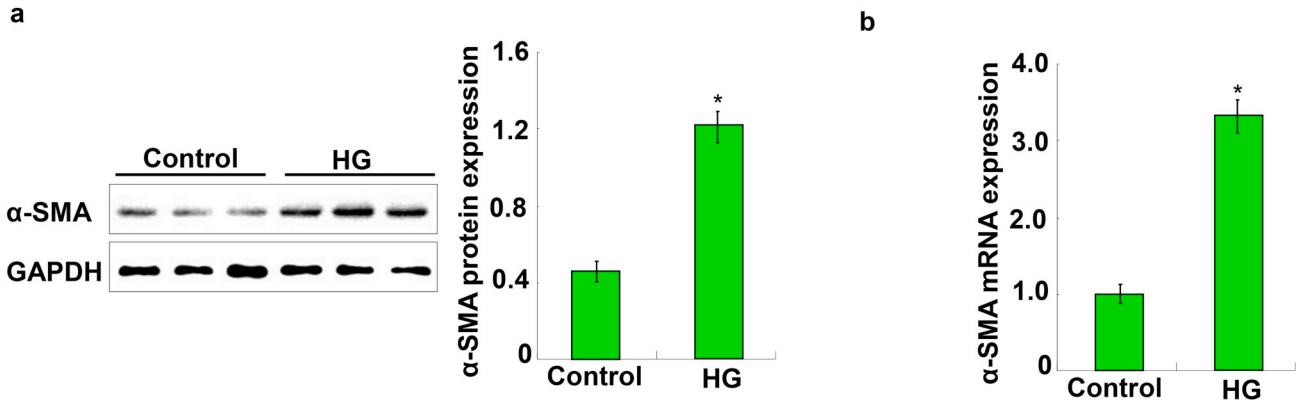

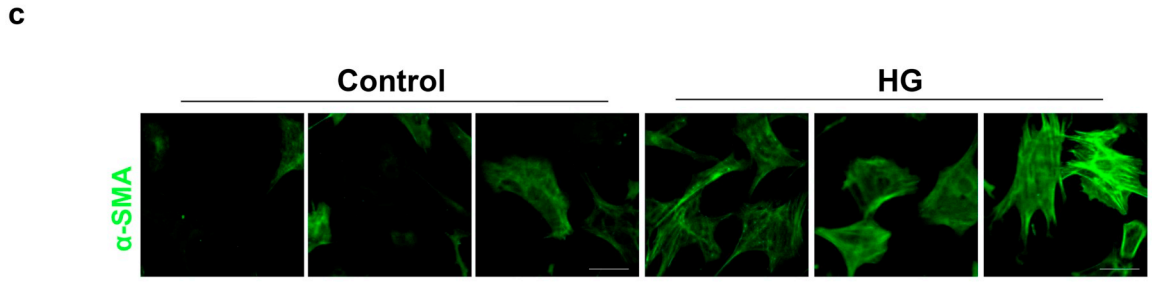

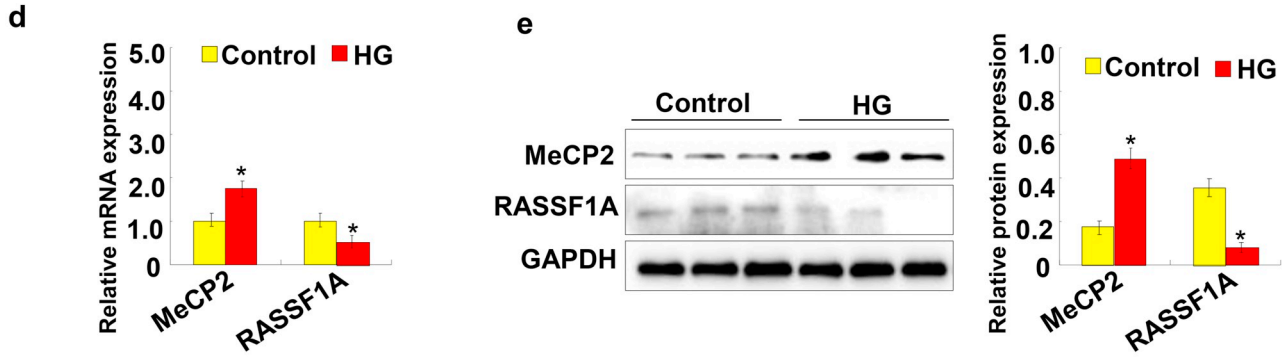

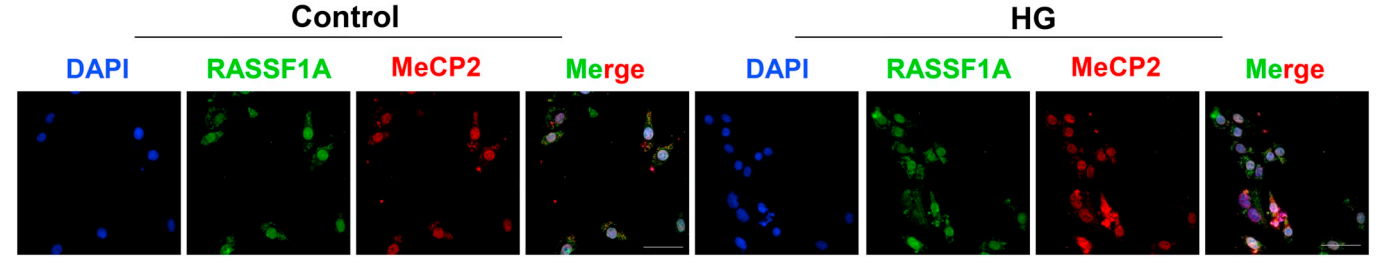

(caption on next page)

Fig. 4. Differential expressions of MeCP2 and RASSF1A in cardiac fibroblast treated by high glucose. (a) The relative protein expression levels of α-SMA in cardiac fibroblast treated by glucose were detected by western blotting. (b) The relative mRNA expression levels of α-SMA in cardiac fibroblast treated by glucose were detected by qRT-PCR. (c) Immunofluorescence analysis was conducted to detect the expression of α-SMA in cardiac fibroblast treated by glucose. α-SMA, green. Scale bar, 50 μm. (d) The relative mRNA expression levels of MeCP2 and RASSF1A in cardiac fibroblast treated by glucose were detected by qRT-PCR. (e) The relative protein expression levels of MeCP2 and RASSF1A in cardiac fibroblast treated by glucose were detected by western blotting. (f) Immunofluorescence showing the relative protein expression levels of MeCP2 and RASSF1A in cardiac fibroblast treated by glucose. RASSF1A, green; MeCP2, red; nuclei, blue. Scale bar, 50 μm. Data are representative of at least three separate experiments. *$p < .05$, **$p < .01$ vs vehicle or control. (For interpretation of the references to colour in this figure legend, the reader is referred to the web version of this article.)

We set out to validate the fibrosis by detecting the expression of protein markers of fibrosis. Hematoxylin and eosin (H&E) and Sirius-red staining indicated that morphological abnormalities and fibrosis were observed in DCM hearts (Fig. 1a, b). Masson Trichrome Stain was used to identify areas of collagen deposition by the blue colour (Fig. 1c). Collagen accumulation was significantly increased in the DCM groups compared to the control groups (Fig. 1c). Moreover, the CollagenIand α-SMA mRNA and protein expressions increased in the DCM groups compared to the control groups (Fig. 1d, e, f). These results led us to speculate that fibrosis might play a crucial role in inducing DCM.

3.2. STZ-induced rat display symptoms of DCM and fibrosis

We next detected the expression of protein markers of fibrosis in STZ-induced rat DCM. Moreover, Hematoxylin and eosin (H&E) and Sirius-red staining indicated that morphological abnormalities and fibrosis were observed in STZ-induced DCM hearts (Fig. 2a, b). Masson Trichrome Stain was used to identify areas of collagen deposition by the blue colour in the STZ-induced DCM hearts (Fig. 2c). Moreover, the CollagenIand Collagen III mRNA and protein expressions increased in the STZ groups compared to the control groups (Fig. 2 d, e, f). These results showed that DCM showed marked increase of the fibrosis in STZ rats.

3.3. Differential expression of MeCP2 and RASSF1A in DCM patient and STZ-induced DCM hearts

To evaluate the functional significance of MeCP2 and RASSF1A in DCM patient and STZ-induced rat DCM. We found that the level of MeCP2 was significantly increased in the DCM patient, whereas RASSF1A was significantly decreased in the DCM patient (Fig. 3a, b, c). Moreover, MeCP2 was significantly increased in the STZ-induced DCM hearts, whereas RASSF1A was significantly decreased in the STZ-induced DCM hearts (Fig. 3d, e, f). All these results suggest that elevated MeCP2 and down regulated RASSF1A was found in DCM patient and STZ-induced DCM hearts.

3.4. Differential expression of MeCP2 and RASSF1A in cardiac fibroblast treated by glucose

We wanted to confirm our observations in cultured cardiac fibroblast treated by high glucose, which would also allow us to decipher the underlying mechanisms. It is known that cardiac fibroblast treated with high glucose was induced cardiac fibroblast activation. Results indicated that the expression of α-SMA level was increased in activated cardiac fibroblast compared with cardiac fibroblast untreated with high glucose (Fig. 4a, b, c). However, the expression of MeCP2 was increased, RASSF1A level was decreased in activated cardiac fibroblast compared with cardiac fibroblast untreated with high glucose (Fig. 4d, e, f).

3.5. Knockdown of MeCP2 inhibits HG-induced cardiac fibroblasts proliferation

To further explore the role of MeCP2 in cardiac fibroblasts proliferation. In our study, we exposed cardiac fibroblasts to HG, which is known to induce fibroblast activation in vitro. The expression of MeCP2 significantly decreased in the cardiac fibroblasts transfected with

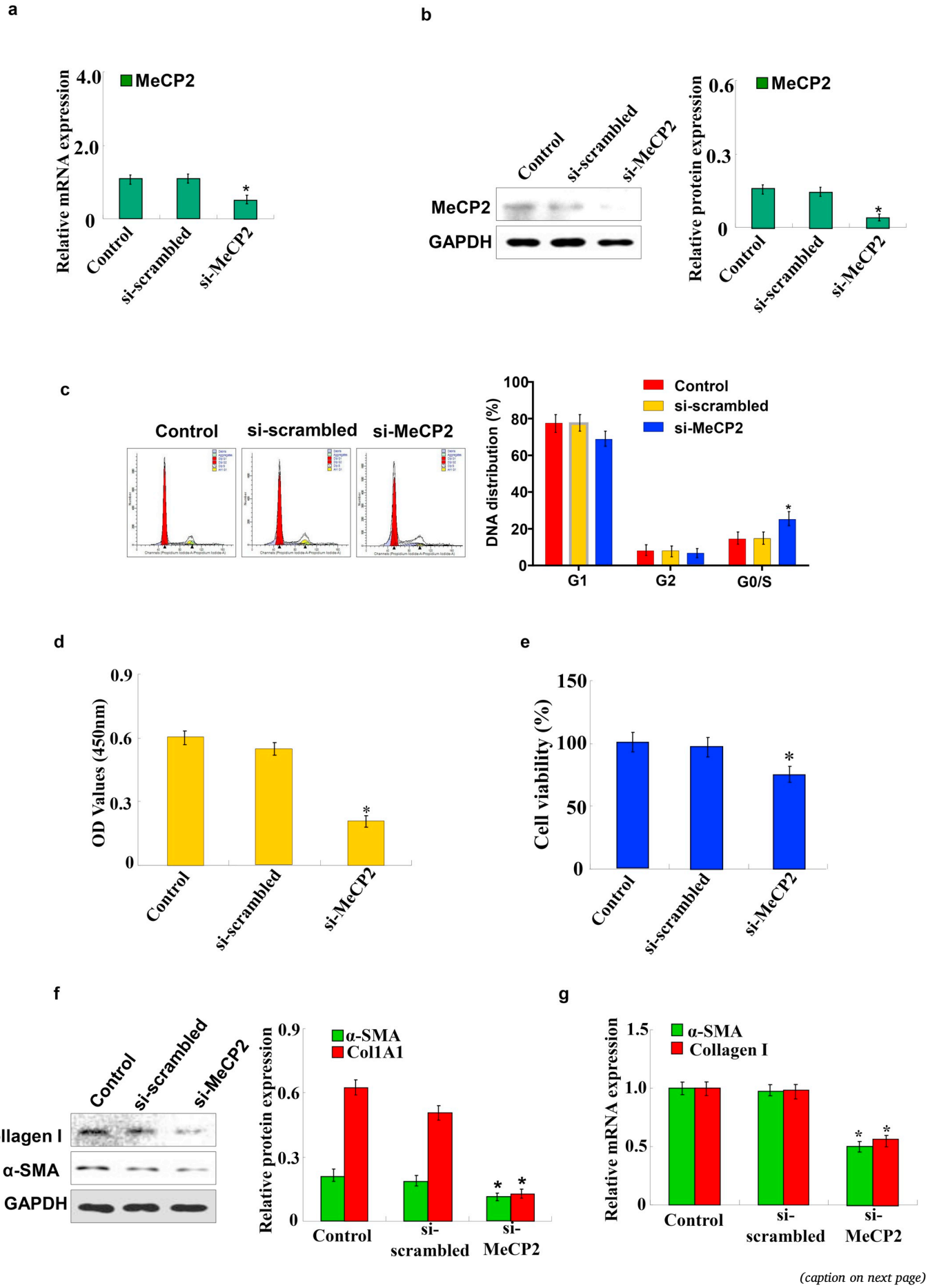

(caption on next page)

Fig. 5. Knockdown of MeCP2 inhibits high glucose-induced cardiac fibroblasts proliferation. (a) Cardiac fibroblasts transfected with siRNA-MeCP2 or control siRNA-scrambled, after transfection. The relative mRNA expression levels of MeCP2 were detected by qRT-PCR. (b) The relative protein expression levels of MeCP2 were detected by western blotting. (c) Cardiac fibroblasts transfected with siRNA-MeCP2 or control siRNA-scrambled, after transfection. Then cells were harvested and the cell-cycle distribution was analyzed by Flow cytometry analysis. (d) Cardiac fibroblasts transfected with siRNA-MeCP2 or control siRNA-scrambled, after transfection. Then cell proliferation was measured by CCK-8 assay. (e) Cardiac fibroblasts transfected with siRNA-MeCP2 or control siRNA-scrambled, after transfection. Then cell proliferation was measured by MTT assay. (f) Cardiac fibroblasts transfected with siRNA-MeCP2 or control siRNA-scrambled, after transfection. The relative protein expression levels of CollagenIand α-SMA were detected by western blotting. (g) The relative mRNA expression levels of CollagenIand α-SMA were detected by qRT-PCR. Data are representative of at least three separate experiments. *$p < .05$, **$p < .01$ vs vehicle or scrambled.

siRNA-MeCP2 (Fig. 5a, b). Treatment of cardiac fibroblasts with siRNA-MeCP2 had a profound inhibitory effect on HG-induced cardiac fibroblasts proliferation (Fig. 5c, d, e). Induction of Collagen I and α-SMA gene expression are classic events associated with fibroblasts proliferation; both were repressed in siRNA-MeCP2 treated cultures (Fig. 5f, g).

3.6. MeCP2 suppression of RASSF1A expression in HG-induced cardiac fibroblasts

To determine whether MeCP2 suppression of RASSF1A expression in HG-induced cardiac fibroblasts, cardiac fibroblasts transfected with siRNA-MeCP2, The expression levels of MeCP2 decreased significantly in the siRNA-MeCP2 group, while the levels of RASSF1A increased (Fig. 6a, b, c). In addition, our study found that the expression levels of RASSF1A in the 5-AzadC-treated cardiac fibroblasts increased to the only HG-treated cardiac fibroblasts (Fig. 6d, e). However, the expression levels of MeCP2 increased significantly in the MeCP2 over expression group, while the levels of RASSF1A decreased (Fig. 6f, g, h). The results suggested which demonstrated that MeCP2 inhibits RASSF1A expression in HG-induced cardiac fibroblasts.

3.7. RASSF1A mediated ERK1/2 triggers HG-induced cardiac fibroblasts proliferation

Due to RASSF1A can regulate Ras/ERK1/2 pathway negatively, we detected the effect of RASSF1A on the Ras/ERK1/2 pathway. ERK1/2 is a downstream factor in Ras signaling. Elevated p-ERK1/2 was discovered in DCM heart tissue and HG-induced cardiac fibroblasts (Fig. 7a, b, c), while decreased RASSF1A expression was found. Furthermore, cardiac fibroblast was transfected at high efficiency with a siRNA-MeCP2 and 5-AzadC. The up regulation of RASSF1A was induced by 5-AzadC treated; however, the protein level of p-ERK1/2 was decreased by 5-AzadC treated compared to untreated cardiac fibroblasts (Fig. 7d). Cardiac fibroblasts transfected with siRNA-MeCP2 expressed lower levels of p-ERK1/2 protein, while cardiac fibroblasts transfected with pEGFP-C1-MeCP2 expressed higher levels of p-ERK1/2 protein (Fig. 7e). Furthermore, the expression of RASSF1A significantly decreased in the cardiac fibroblasts transfected with siRNA-RASSF1A, while the protein level of p-ERK1/2 was increased (Fig. 7f). Treatment of cardiac fibroblasts with siRNA-RASSF1A had a significant promotion effect on HG-induced cardiac fibroblasts proliferation (Fig. 7g, h). These data indicate that MeCP2 promotes cardiac fibroblasts proliferation and DCM by suppression of RASSF1A/ERK1/2.

4. Discussion

In diabetes mellitus (DM), the metabolic environment of hyperglycemia causes cardiac fibroblast activation leading to diabetic cardiomyopathy (DCM), an independent cause of cardiac fibrosis [18]. Excessive deposition of extracellular matrix (ECM), such as collagens plays a key role in the process of cardiac fibrosis [19]. Our study suggests that HG induces DCM and cardiac fibroblast proliferation, which is partially mediated by a MeCP2 suppression of RASSF1A mechanism. Cardiac fibroblast serves as an essential quality control mechanism to maintain the function of heart during DCM [20]. The abnormal of

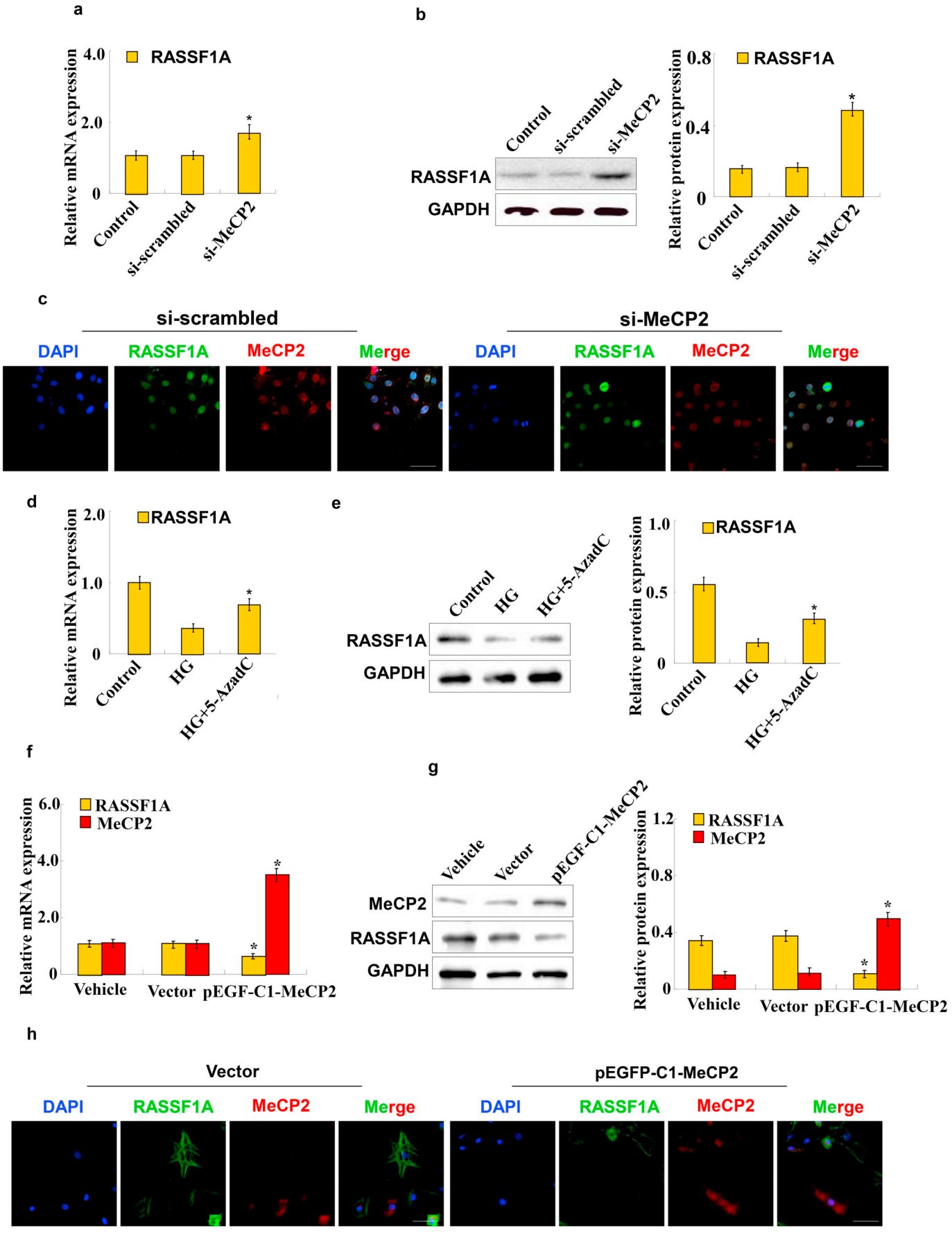

(caption on next page)

Fig. 6. MeCP2 suppression of RASSF1A expression in high glucose-induced cardiac fibroblasts. (a) Cardiac fibroblasts transfected with siRNA-MeCP2 or control siRNA-scrambled, after transfection. The relative mRNA expression levels of RASSF1A were detected by qRT-PCR. (b) The relative protein expression levels of RASSF1A were detected by western blotting. (c) Immunofluorescence showing the relative protein expression levels of MeCP2 and RASSF1A in cardiac fibroblast transfected with siRNA-MeCP2 or control siRNA-scrambled. RASSF1A, green; MeCP2, red; nuclei, blue. Scale bar, 50 μm. (d) Cardiac fibroblasts treated with glucose and 5-azadC, the relative mRNA expression levels of RASSF1A were detected by qRT-PCR. (e) Cardiac fibroblasts treated with glucose and 5-azadC, the relative protein expression levels of RASSF1A were detected by western blotting. (f) Cardiac fibroblasts transfected with pEGFP-C1-MeCP2, the relative mRNA expression levels of MeCP2 and RASSF1A were detected by qRT-PCR. (g) Cardiac fibroblasts transfected with pEGFP-C1-MeCP2, the relative protein expression levels of MeCP2 and RASSF1A were detected by western blotting. (h) Cardiac fibroblasts transfected with pEGFP-C1-MeCP2, Immunofluorescence showing the relative protein expression levels of MeCP2 and RASSF1A in cardiac fibroblast transfected with siRNA-MeCP2 or control siRNA-scrambled. RASSF1A, green; MeCP2, red; nuclei, blue. Scale bar, 50 μm. Data are representative of at least three separate experiments. *$p < .05$, **$p < .01$ vs vector or scrambled; $^{\#}p < .05$, $^{\#\#}p < .01$ vs Model (High glucose) (For interpretation of the references to colour in this figure legend, the reader is referred to the web version of this article.)

cardiac fibroblast proliferation induces heart dysfunction and ECM deposition, thereby exacerbating the development of DCM.

Our results suggest that collagen accumulation in STZ-induced experimental DCM rats and DCM patient. In this study, we proved that the expression of the MeCP2 was up regulated in the DCM patients, HG-treated cardiac fibroblast and STZ-induced DCM rat heart tissue, while RASSF1A was decreased. Recent studies reported that epigenetic gene regulation has been recognized to play a crucial role in cardiac fibrosis [21,22]. MeCP2 as a global repressor of transcription, acting by binding to the methylated sequences of its target gene promoters and recruiting transcriptional repressors to silence gene expression [23]. Emerging studies have revealed that MeCP2 is vital in many diseases, especially in cardiovascular diseases, such as cardiac arrhythmogenesis [24]. However, there have been no reports about MeCP2 and cardiac fibroblast activation in DCM.

What is more, we demonstrated that siRNA-MeCP2 treated cardiac fibroblasts reduced cardiac fibroblasts cell proliferation activity. Down regulation of MeCP2 in cardiac fibroblasts also inhibited collagen I and α-SMA gene expression. Furthermore, elevated RASSF1A was found in the siRNA-MeCP2 and 5-AzadC-treated cardiac fibroblasts, while over expression of MeCP2 down regulated RASSF1A expression.

Given RASSF1A can negatively regulate Ras/ERK1/2 pathway [25], confirming previous studies that suggested a prominent role of Ras/ERK1/2 signaling in fibrosis and proliferation [26]. Elevated p-ERK1/2 was discovered in DCM heart tissue and HG-induced cardiac fibroblasts, while decreased RASSF1A expression was found. Furthermore, the level of p-ERK1/2 was decreased by 5-AzadC and siRNA-MeCP2 treated cardiac fibroblasts, while the level of p-ERK1/2 was increased by MeCP2 over expression vector treated cardiac fibroblasts. In addition, the expression of RASSF1A significantly decreased in the cardiac fibroblasts transfected with siRNA-RASSF1A, while the protein level of p-ERK1/2 was increased. Treatment of cardiac fibroblasts with siRNA-RASSF1A promotes cardiac fibroblasts proliferation.

To our knowledge, this may be the first report of MeCP2 triggers diabetic cardiomyopathy and cardiac fibroblast proliferation by suppressing RASSF1A/ ERK1/2. Future studies are needed to elucidate the utility of MeCP2 as diagnostic markers to predict DCM and the possible therapeutic target in the progression of DCM.

Author contributions

HT and XSD conceived and designed the experiments, and discussed the results. HT, JYT and PS carried out all experiments. ZYD and PS helped with the human heart biopsy specimen. ZYS and QW supported with data presentation and in manuscript revision. HT and XSD wrote the manuscript, which was read, edited and approved by all the authors.

Declaration of Competing Interest

There are none.

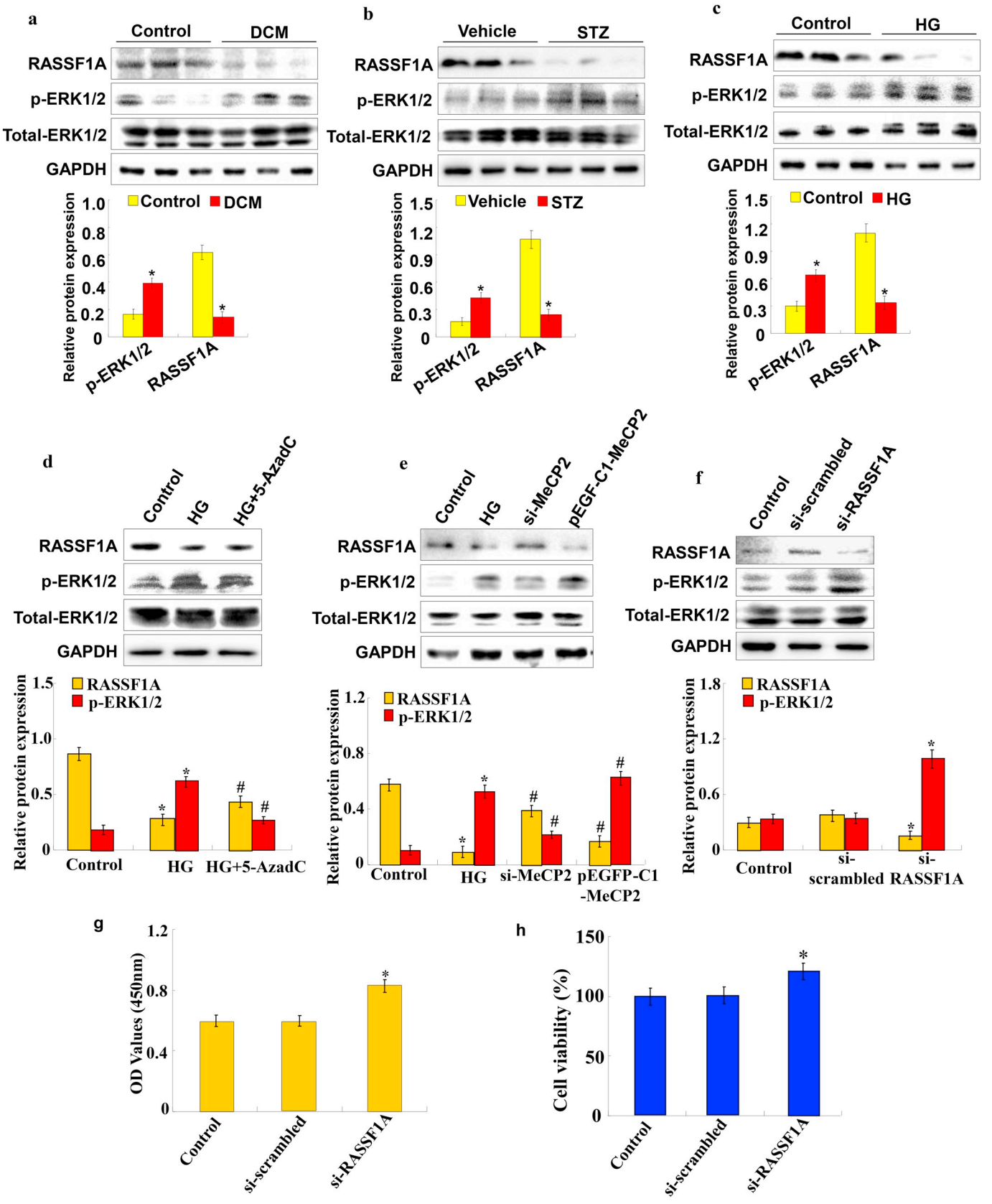

(caption on next page)

Fig. 7. RASSF1A mediated ERK1/2 triggers high glucose-induced cardiac fibroblasts proliferation. (a) The relative RASSF1A and p-ERK1/2 protein expression levels in DCM patient were detected by Western blotting. (b) The relative RASSF1A and p-ERK1/2 protein expression levels in STZ-induced rat DCM were detected by Western blotting. (c) The relative RASSF1A and p-ERK1/2 protein expression levels in cardiac fibroblast treated by glucose were detected by Western blotting. (d) Cardiac fibroblasts treated with glucose and 5-azadC, the relative protein expression levels of RASSF1A and p-ERK1/2 were detected by western blotting. (e) Cardiac fibroblasts transfected with pEGFP-C1-MeCP2 and siRNA-MeCP2, the relative protein expression levels of RASSF1A and p-ERK1/2 were detected by western blotting. (f) Cardiac fibroblasts transfected with siRNA-RASSF1A or control siRNA-scrambled. The relative protein expression levels of RASSF1A and p-ERK1/2 were detected by western blotting. (g) Cardiac fibroblasts transfected with siRNA-RASSF1A or control siRNA-scrambled. Then cell proliferation was measured by CCK-8 assay. (h) Cardiac fibroblasts transfected with siRNA-RASSF1A or control siRNA-scrambled. Then cell proliferation was measured by MTT assay. Data are representative of at least three separate experiments. *$p < .05$, **$p < .01$ vs Control (Vehicle), $^{\#}p < .05$, $^{\#\#}p < .01$ vs Model (High glucose)

Acknowledgements

This project was supported by National Natural Science Foundation of China (81700212, 81873131) and Natural Science Foundation of Anhui Provincial (1808085MH231) and Natural Science Foundation of Anhui Provincial Education Department (KJ2017A168).

References

[1] A.C. Armstrong, B. Ambale-Venkatesh, E. Turkbey, S. Donekal, E. Chamera, J.Y. Backlund, P. Cleary, J. Lachin, D.A. Bluemke, J.A. Lima, Diabetes Care 40 (2017) 405–411.
[2] E. Villalobos, A. Criollo, G.G. Schiattarella, F. Altamirano, K.M. French, H.I. May, N. Jiang, N.U.N. Nguyen, D. Romero, J.C. Roa, L. Garcia, G. Diaz-Araya, E. Morselli, A. Ferdous, S.J. Conway, H.A. Sadek, T.G. Gillette, S. Lavandero, J.A. Hill, Circulation 139 (20) (2019) 2342–2357.
[3] I. Valiente-Alandi, S.J. Potter, A.M. Salvador, A.E. Schafer, T. Schips, F. Carrillo-Salinas, A.M. Gibson, M.L. Nieman, C. Perkins, M.A. Sargent, J. Huo, J.N. Lorenz, T. DeFalco, J.D. Molkentin, P. Alcaide, B.C. Blaxall, Circulation 138 (2018) 1236–1252.
[4] D. Cervantes, C. Crosby, Y. Xiang, Circ. Res. 106 (2010) 79–88.
[5] Z. Wang, Y. Liu, M. Takahashi, K. Van Hook, K.M. Kampa-Schittenhelm, B.C. Sheppard, R.C. Sears, P.J. Stork, C.D. Lopez, Proc. Natl. Acad. Sci. U. S. A. 110 (2013) 312–317.
[6] Y. Liu, H. Zhu, Z. Su, C. Sun, J. Yin, H. Yuan, S. Sandoghchian, Z. Jiao, S. Wang, H. Xu, Int. Immunol. 24 (2012) 605–612.
[7] M. Ye, T. Huang, C. Ni, P. Yang, S. Chen, EBioMedicine 18 (2017) 32–40.
[8] Y. Ma, Y. Bai, H. Mao, Q. Hong, D. Yang, H. Zhang, F. Liu, Z. Wu, Q. Jin, H. Zhou, J. Cao, J. Zhao, X. Zhong, Biosens. Bioelectron. 85 (2016) 641–648.
[9] X. Kong, J. Chen, W. Xie, S.M. Brown, Y. Cai, K. Wu, D. Fan, Y. Nie, S. Yegnasubramanian, R.L. Tiedemann, Y. Tao, R.W. Chiu Yen, M.J. Topper, C.A. Zahnow, H. Easwaran, S.B. Rothbart, L. Xia, S.B. Baylin, Cancer Cell 35 (4) (2019) 633–648.e7.
[10] A.R. Gliga, K. Engstrom, M. Kippler, H. Skroder, S. Ahmed, M. Vahter, R. Raqib, K. Broberg, Arch. Toxicol. 92 (2018) 2487–2500.
[11] S. Pol Bodetto, D. Carouge, M. Fonteneau, J.B. Dietrich, J. Zwiller, P. Anglard, Neuropharmacology 73 (2013) 31–40.
[12] H. Yin, Y. Zhou, Z. Xu, M. Wang, S. Ai, Biosens. Bioelectron. 49 (2013) 39–45.
[13] J.S. Witteveen, M.H. Willemsen, T.C. Dombroski, N.H. van Bakel, W.M. Nillesen, J.A. van Hulten, E.J. Jansen, D. Verkaik, H.E. Veenstra-Knol, C.M. van Ravenswaaij-Arts, J.S. Wassink-Ruiter, M. Vincent, A. David, C. Le Caignec, J. Schieving, C. Gilissen, N. Foulds, P. Rump, T. Strom, K. Cremer, A.M. Zink, H. Engels, S.A. de Munnik, J.E. Visser, H.G. Brunner, G.J. Martens, R. Pfundt, T. Kleefstra, S.M. Kolk, Nat. Genet. 48 (2016) 877–887.
[14] P.J. Skene, R.S. Illingworth, S. Webb, A.R. Kerr, K.D. James, D.J. Turner, R. Andrews, A.P. Bird, Mol. Cell 37 (2010) 457–468.
[15] R.R. Ram, S. Mendiratta, B.O. Bodemann, M.J. Torres, U. Eskiocak, M.A. White, Mol. Cell. Biol. 34 (2014) 2350–2358.
[16] A. Pang, Y. Hu, P. Zhou, G. Long, X. Tian, L. Men, Y. Shen, Y. Liu, Y. Cui, Cardiovasc. Diabetol. 14 (2015) 134.
[17] Y.S. Yoon, S. Uchida, O. Masuo, M. Cejna, J.S. Park, H.C. Gwon, R. Kirchmair, F. Bahlman, D. Walter, C. Curry, A. Hanley, J.M. Isner, D.W. Losordo, Circulation 111 (2005) 2073–2085.
[18] L. Ji, F. Liu, Z. Jing, Q. Huang, Y. Zhao, H. Cao, J. Li, C. Yin, J. Xing, F. Li, Diabetes 66 (2017) 1586–1600.
[19] I. Russo, M. Cavalera, S. Huang, Y. Su, A. Hanna, B. Chen, A.V. Shinde, S.J. Conway, J.M. Graff, N.G. Frangogiannis, Circ. Res. 124 (8) (2019) 1214–1227.
[20] A. Bugyei-Twum, A. Advani, S.L. Advani, Y. Zhang, K. Thai, D.J. Kelly, K.A. Connelly, Cardiovasc. Diabetol. 13 (2014) 89.
[21] S.C. Mayer, R. Gilsbach, S. Preissl, E.B. Monroy Ordonez, T. Schnick, N. Beetz, A. Lother, C. Rommel, H. Ihle, H. Bugger, F. Ruhle, A. Schrepper, M. Schwarzer, C. Heilmann, U. Bonisch, S.K. Gupta, J. Wilpert, O. Kretz, D. von Elverfeldt, J. Orth, K. Aktories, F. Beyersdorf, C. Bode, B. Stiller, M. Kruger, T. Thum, T. Doenst, M. Stoll, L. Hein, Circ. Res. 117 (2015) 622–633.
[22] H. Tao, Z.Y. Song, X.S. Ding, J.J. Yang, K.H. Shi, J. Li, Endocrine 62 (2018) 281–291.
[23] G. Devailly, M. Grandin, L. Perriaud, P. Mathot, J.G. Delcros, Y. Bidet, A.P. Morel, J.Y. Bignon, A. Puisieux, P. Mehlen, R. Dante, Nucleic Acids Res. 43 (2015) 5838–5854.
[24] J.A. Herrera, C.S. Ward, X.H. Wehrens, J.L. Neul, Hum. Mol. Genet. 25 (2016) 4983–4995.
[25] X. Huang, G. Kong, Y. Li, W. Zhu, H. Xu, X. Zhang, J. Li, L. Wang, Z. Zhang, Y. Wu, X. Liu, X. Wang, Biomed. Pharmacother. 84 (2016) 447–453.
[26] J. Lauriol, K. Keith, F. Jaffre, A. Couvillon, A. Saci, S.A. Goonasekera, J.R. McCarthy, C.W. Kessinger, J. Wang, Q. Ke, P.M. Kang, J.D. Molkentin, C. Carpenter, M.I. Kontaridis, Sci. Signal. 7 (2014) ra100.